Journal of
Water & Climate Change

IWA PUBLISHING

Journal of Water and Climate Change Vol 12 No 6, 2835 doi: 10.2166/wcc.2021.026

Quantitative analysis of the impacts of climate and land-cover changes on urban flood runoffs: a case of Dar es Salaam, Tanzania

Philip Mzava [a,*], Patrick Valimba[b] and Joel Nobert[b]
[a] Department of Civil Engineering, Dar es Salaam Institute of Technology, P.O. Box 2958, Dar es Salaam, Tanzania
[b] Department of Water Resources Engineering, College of Engineering and Technology, University of Dar es Salaam, P.O Box 35131, Dar es Salaam, Tanzania
*Corresponding author. E-mail: pmzava@gmail.com

PM, 0000-0001-8499-9015

ABSTRACT

Over the past half-century, the risk of urban flooding in Dar es Salaam has increased due to changes in land cover coupled with climatic changes. This paper aimed to quantify the impacts of climate and land-cover changes on the magnitudes and frequencies of flood runoffs in urban Dar es Salaam, Tanzania. A calibrated and validated SWAT rainfall-runoff model was used to generate flood hydrographs for the period 1969–2050 using historical rainfall data and projected rainfall based on the CORDEX-Africa regional climate model. Results showed that climate change has a greater impact on change in peak flows than land-cover change when the two are treated separately in theory. It was observed that, in the past, the probability of occurrence of urban flooding in the study area was likely to be increased up to 1.5-fold by climate change relative to land-cover change. In the future, this figure is estimated to decrease to 1.1-fold. The coupled effects of climate and land-cover changes cause a much bigger impact on change in peak flows than any separate scenario; this scenario represents the actual scenario on the ground. From the combined effects of climate and land-cover changes, the magnitudes of mean peak flows were determined to increase between 34.4 and 58.6% in the future relative to the past. However, the change in peak flows from combined effects of climate and land-cover changes will decrease by 36.3% in the future relative to the past; owing to the lesser variations in climate and land-cover changes in the future compared with those of the past.

Key words: climate, Dar es Salaam, flood frequency, land cover, RCM, SWAT

HIGHLIGHTS

- Investigate temporal variability of urban flood runoffs from the impacts of climate and land-cover changes.
- Compare past and future peak flow trend magnitudes based on CORDEX-Africa RCM under RCP4.5.
- Investigate changes in the historical and future intensities of urban flood runoffs.
- Illustrate the probabilistic impacts of climate and land-cover changes on the recurrence intervals of urban floods.

GRAPHICAL ABSTRACT

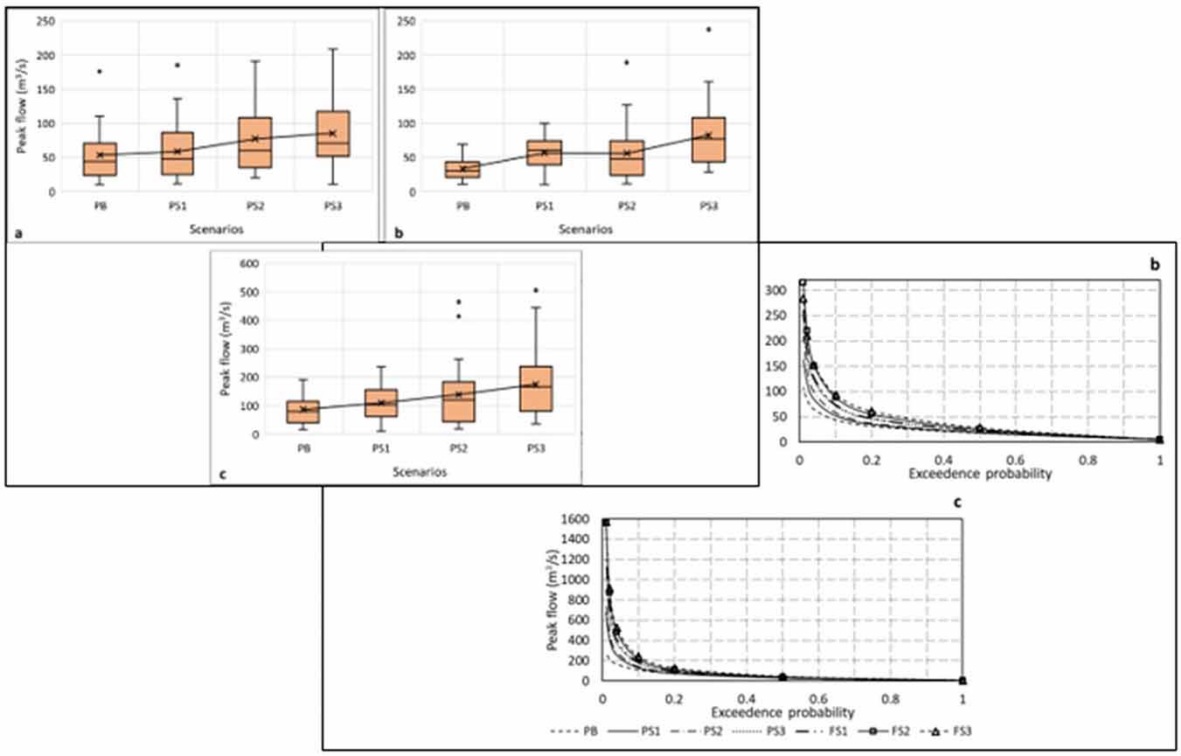

INTRODUCTION

In recent years, urban flooding has become one of the major global environmental hazards (Wakuma *et al.* 2009; Abidin *et al.* 2015). Urban floods can result in a considerable amount of socio-economic adversities, which may include death, destruction of urban infrastructure, and disruption of economic and social services (e.g. power supply, communication, transportation, sewerage, etc.; Hlodversdottir *et al.* 2015; Wu *et al.* 2017). The risk of flooding in urban areas is exacerbated by rapid population growth, high population density, rapid land-use/cover change (urbanization), and climate change (Poelmans *et al.* 2011). Among these various factors, the two most influential ones contributing to urban flooding are climate change and urbanization (Wu *et al.* 2017). Climate change affects the patterns of rainfall extremes and thus exerts direct impacts on surface runoff, flood frequency, and magnitudes. While population and economic growth are considered the lead factors behind urbanization, resulting in an increase of impervious surfaces and socio-economic vulnerability to flooding in urban areas (Mahmoud & Gan 2018).

Among the top ten natural disasters that threaten the economy of Tanzania, flooding ranks second after epidemics (Ngailo *et al.* 2016). In particular, the city of Dar es Salaam has experienced increased cases of flooding in recent years, namely 2007, 2011, 2014, 2015, 2018, 2019, and 2020. There appears to be a temporal increase in the frequency of flooding in the urban area of Dar es Salaam. Being the largest commercial, industrial and urban center of Tanzania contributing to approximately 16% of the country's gross domestic product, events of flooding in the city of Dar es Salaam come with major socio-economic implications. The profound negative impacts of urban flooding in Dar es Salaam are due to the fast-growing population, the existing high population density (>3,100 people/km^2), and rapid urbanization. It is estimated that about 70% of the total population in the region are living in unplanned areas (Kebede & Nicholls 2011). Households' losses following the floods of April 2018 in Dar es Salaam were estimated to be more than $100 million (Erman *et al.* 2019). The occurrence of a temporal shift in both land-use/cover and climate (particularly rainfall) has been reported in the Dar es Salaam urban area by several previous studies. Dar es Salaam urban land cover was observed to be greatly modified since 1979; turning from thick vegetated land toward becoming a barren land (Mzava *et al.* 2019). This change was observed to be continuous, and about 66.1% of the urban area will consist of built-up land cover by 2030. Moreover, the intensity of future extreme rainfall

was observed to increase approximately between 20 and 25% relative to the past. The frequency of extreme rainfall events was also observed to be increasing. These reported changes were said to likely lead to more severe floods in the Dar es Salaam urban area (Mzava *et al.* 2020).

The separate and combined influences of land use/cover and climate changes on surface runoff have been investigated by several previous studies under both historical and future conditions, including Ouellet *et al.* (2012), Chen & Yu (2015), Mallakpour & Villarini (2016), Thanvisitthpon *et al.* (2018), and Akter *et al.* (2018). The effect of land-use/cover change on flood characteristics was observed to be more noticeable for moderate storms, and the impact is reduced during extreme rainfall events (Chen & Yu 2015). This observation was also supported by the findings of Poelmans *et al.* (2011). The influence of climate change on floods was found to be greater than that of land-use/cover change by Notter *et al.* (2007) and Akter *et al.* (2018). It has also been observed that changes in climate significantly affect the frequency and peaks of floods (Ouellet *et al.* 2012). The assessment of the combined effects of climate and land-use/cover changes from the few available studies generally agrees with the theory that flood magnitudes increase with the increase in catchment's impervious area (Chen & Yu 2015; Emam *et al.* 2016). Although the precise effects of climate and land-cover/use changes on urban flooding are difficult to predict, various studies have projected an increase in urban flood risks from rapid land-use/cover change coupled with climate change (Poelmans *et al.* 2011; Akter *et al.* 2018; Jiang *et al.* 2018; Zhou *et al.* 2018). Akter *et al.* (2018) projected a higher contribution of climate change to peak flow in the future compared with urbanization. Contrary to most studies, Rukundo & Dogan (2016) suggested that land-use change impacts predominate the climate change impacts in overall assessment on flood peaks in Kigali, Rwanda.

In this study, a SWAT rainfall-runoff model was developed, calibrated, validated, and used to generate flood hydrographs for the period 1969–2050 using historical climatic data from four gauging stations (Figure 1), and projected climatic data based on the Coordinated Regional Climate Downscaling Experiment (CORDEX)-Africa regional climate model (extracted at the same coordinates as the ground stations). Due to the lack of previous studies on the assessment of flood magnitudes as influenced by climate and land-cover changes in urban areas of Tanzania, the objective of this research is to quantify the independent and combined impacts of climate and land-cover changes on the magnitudes and frequencies of flood runoffs in urban Dar es Salaam. Considering the reported increase in extreme rainfall intensities and frequencies in urban Dar es Salaam, and the ongoing urban development and infrastructural upgrading projects, these changes could have direct and

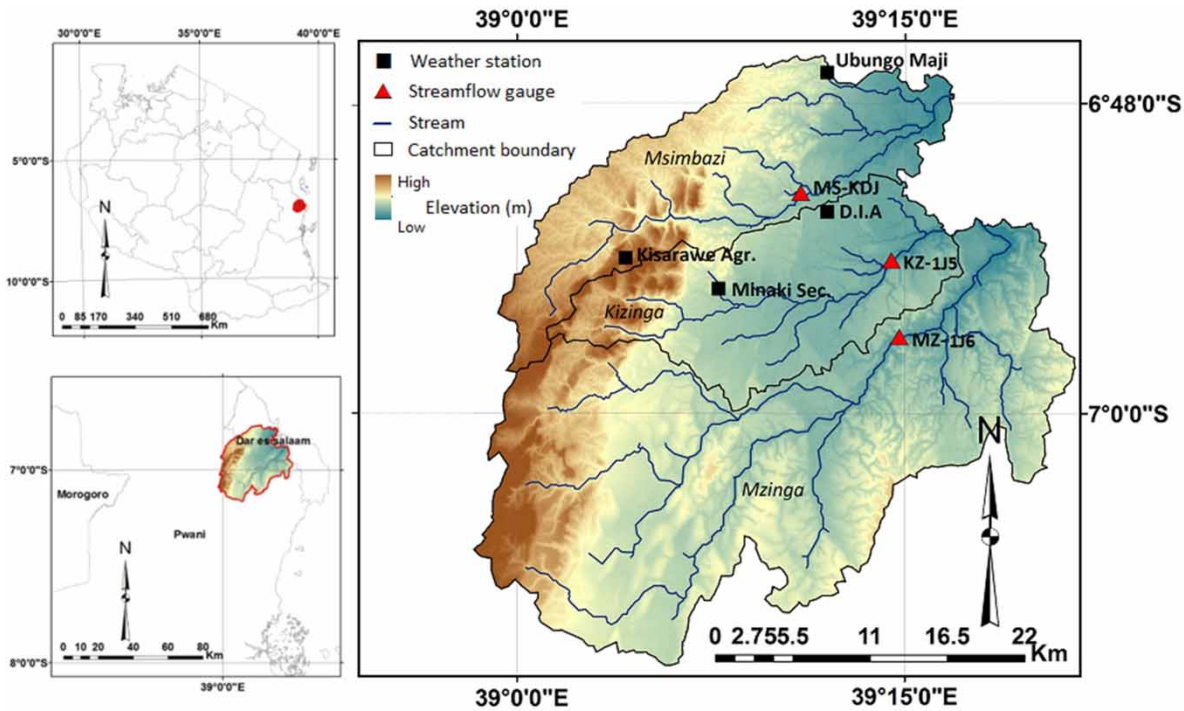

Figure 1 | Details of the study area.

significant influences on flooding in the study area. Therefore, understanding the separate and combined impacts of climate and land-cover changes on flood runoffs from this research is considered significant and valuable information to the design and practice of hydrologic engineering in the study area.

DATA AND METHODOLOGY

Study area

The study was carried out in the selected 1,200 km^2 study area which is located within Pwani and Dar es Salaam regions in the eastern coastal part of Tanzania, between longitudes 39°01′18.37″–39°28′29.55″ E and latitudes 6°35′17.48″–7°59′18.92″ S. The area consists of Msimbazi (265.5 km^2), Kizinga (247.1 km^2), and Mzinga (686.4 km^2) subcatchments; reaching 40.2, 29.1, and 58.2 km, respectively, starting from the highlands of the Pwani region, running through the central urban portion of the Dar es Salaam region, and draining the water into the Indian Ocean (Figure 1). Within the study area, the highlands of Pwani are approximately 240 m above sea level; with a peak altitude of 339 m, and receive an average of 1,200 mm of rainfall annually. The lowlands of the Dar es Salaam region are approximately 57 m above sea level; with the lowest altitude of 15 m, and receive an average of 1,000 mm of rainfall annually. The area has a bi-modal rainfall distribution, the two main rainy seasons being the long rains and the short rains. The long rains season (*Masika*) occurs from mid-March to the end of May and the short rains (*Vuli*) from mid-October to late December. The study area is characterized by tropical climatic conditions. It is generally hot and humid throughout the year with mean daily temperature ranging from 26 °C during the coolest season (June–September) to 35 °C during the hottest season (October to March) (Mahongo & Khamis 2006).

Data availability and properties

The data used in this study included topography data, land-cover data, soil data, streamflow data, rainfall, and other climatic data. These data were collected from different sources as elaborated in this section. The land-cover digital models of the study area generated by Mzava *et al.* (2019) (of historical years 1979, 2014, and the projected scenario of the year 2030) were used as input data when carrying out hydrological modeling in this study. Five major land-cover classes were identified by Mzava *et al.* (2019), including *grassland*, *forest*, *bare land*, *medium/low-density built-up area*, and *high-density built-up area*. Based on Mzava *et al.* (2019), an additional scenario of projected land-use/cover for the year 2046 was generated in this study in an effort to have a more representative scenario in the estimation of future peak flow magnitudes; as will be seen in the subsequent sections. Generally, over time, the land cover of the study area was observed to shift from vegetated land toward becoming more of a built-up area (Figure 2(a)). Using the curve number (CN) metric, the imperviousness of the study area was observed to gradually increase with time (Figure 2(a)). The overall CN value of the study area estimated using the area-weighted average method, based on the land-cover type, the hydrologic soil group, and the normal antecedent moisture conditions (AMCII), was found to change from 72 in 1979 to 93 in 2046.

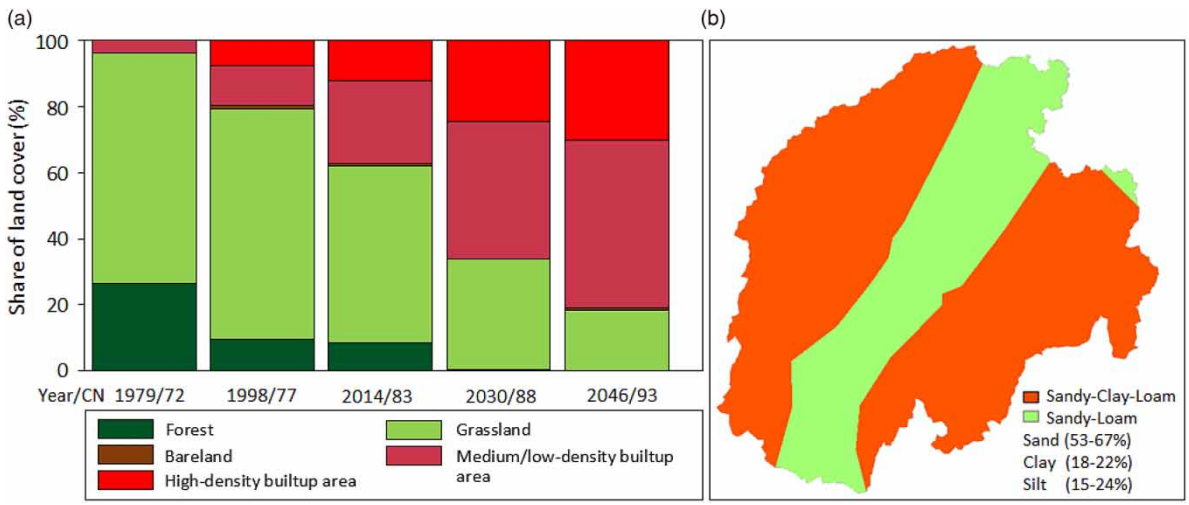

Figure 2 | (a) Temporal shift in the proportions of land covers, (b) soil types and distribution.

A 1-km spatial resolution digital soil map was extracted from the harmonized world soil database (Dewitte *et al.* 2013), which was established by the Food and Agriculture Organization (FAO) in collaboration with the International Institute for Applied System Analysis (IIASA). The soil data indicated the predominance of sandy–clay–loam and sandy–loam soils in the study area. Particle distribution showed that on average, sand is more dominant (61%) in the study region, while clay (19%) and silt (20%) were found to be in moderate and near-equal proportions (Figure 2(b)).

Topographic data of the study area was extracted from a 30-m resolution Digital Elevation Model (DEM) downloaded from the Shuttle Radar Topography Mission (SRTM) database (http://srtm.csi.cgiar.org/). Historical rainfall records of daily time step of four ground-based gauging stations (Figure 1) were obtained from the archives of the Tanzania Meteorological Agency (TMA) for the period 1967–2017. The CORDEX repository for the Africa domain (AFR-44) Regional Climate Model (RCM) (available at: https://esgf-node.llnl.gov/search/esgf-llnl/) was used to obtain future records of rainfall and other climatic data (including *wind speed*, *relative humidity*, *maximum and minimum temperature*, and *solar radiation*) of daily time step for the period 2018–2050. Descriptive statistics of daily climatic data used in this study (averaged over the entire study period and spatial extent) are presented in Table 1.

The Representative Concentration Pathway (RCP) 4.5 was used as the criterion for selecting the RCM future daily climatic data. The RCP4.5 medium-level concentration scenario of greenhouse gas was used because it is considered a more realistic projection scenario as suggested by Wang *et al.* (2017) and Hausfather & Peters (2020). The coordinates of the ground-based weather stations in the study area were used in the extraction of the projected RCM climatic data. The Delta method was then used in the bias correction of the RCM output while attempting to obtain a more realistic climate projection by representing the effects of the local forcings. Trzaska & Schnarr (2014) and Yazd *et al.* (2019) discuss the Delta method in detail, including its merits and shortcomings compared with other methods of statistical downscaling.

Historical climatic records of *wind speed*, *relative humidity*, *solar radiation*, and *temperature* (maximum and minimum) from Dar es Salaam International Airport (DIA) were obtained from TMA. A weather generator was developed based on these historical climatic records from the DIA station and was then used for filling the gaps in the climatic data. Historical records of daily streamflow for the period 1969–1972 of two flow gauging stations, i.e. Kizinga at Buza (KZ-1J5) and Mzinga at Majimatitu (MZ-1J6), were obtained from the Wami-Ruvu River Basin Water Office (WRRBWO) of the Tanzania Ministry of Water.

Hydrological modeling

In this study, the volume of surface runoff was estimated using the Soil Conservation Service-Curve Number (SCS-CN) method (USDA 1972), also called the runoff curve number method. The SCS-CN method is a well-established method in hydrologic engineering for the estimation of direct runoff from storm rainfall. The popularity of the SCS-CN method is because of its convenience, simplicity, and responsiveness to the four watershed properties, i.e. soil type, land use/cover, surface condition, and antecedent moisture condition (Ponce & Hawkins 1996). The SCS-CN method takes the form:

$$Q_{\text{surf}} = (P_{\text{i}} - I_{\text{a}})^2/(P_{\text{i}} - I_{\text{a}} + S) \quad \text{for } I_{\text{a}} \le P, \text{ otherwise } Q_{\text{surf}} = 0 \tag{1}$$

$$I_{\text{a}} = \lambda S \tag{2}$$

$$S = 25.4(1000/\text{CN} - 10) \tag{3}$$

where Q_{surf} is the direct runoff, P_{i} is the rainfall depth for the day, I_{a} is the initial abstraction, S is the potential maximum retention, which ranges between 0 and ∞, λ is the initial abstraction coefficient, and CN is the curve number, a non-dimensional quantity varying between 0 and 100. Higher CN values indicate high runoff potential. Except for λ and CN which are unitless, the remaining variables are in millimeters (mm). I_{a} includes short-term losses due to evaporation, interception, infiltration, and surface detention. The SCS has adopted a standard value of 0.2 for λ (SCS 1985), although this can be estimated by calibration with field data. S characterizes the watershed's potential for abstracting and retaining storm moisture, it is related to land use/cover, soil infiltration, and the antecedent moisture condition of the watershed through CN.

In this study, the SCS-CN method and hydrological modeling, in general, were performed by using the Soil and Water Assessment Tool (SWAT; Arnold *et al.* 1998), using the QSWAT plugin version 1.4 within the QGIS 2.6.1 (more details can be found at http://qgis.org/en/docs/index.html) interface. SWAT is a spatially semi-distributed, time-continuous, and physically based hydrologic model developed by the Agricultural Research Service of the United States Department of

Table 1 | Descriptive statistics of climatic data

	Jan	Feb	Mar	Apr	May	Jun	Jul	Aug	Sep	Oct	Nov	Dec
T_{max} (°C)	32.08	32.59	32.27	30.87	30.11	29.56	29.28	29.71	30.55	31.28	31.65	31.88
T_{min} (°C)	23.94	23.73	23.15	22.66	21.49	19.47	18.49	18.42	18.78	20.20	21.83	23.37
Std. dev._T_{max}	1.35	1.35	1.77	1.93	1.66	1.25	1.25	1.33	1.24	1.33	1.33	1.44
Std. dev._T_{min}	1.70	1.67	1.37	0.89	1.25	1.53	1.49	1.38	1.45	1.61	1.59	1.72
Total rainfall (mm)	65.05	56.71	145.50	260.55	170.81	38.34	20.91	21.59	23.57	61.34	119.61	112.79
Std. dev._Total rain	7.97	8.51	10.61	15.07	12.57	5.05	2.69	2.92	3.52	7.57	11.74	10.66
Skewness_Total rain	7.50	6.40	3.75	3.12	3.90	6.94	8.96	7.35	8.80	6.14	5.09	6.06
Rainy days (num.)	7.88	5.12	13.70	19.56	14.81	6.28	5.70	5.72	5.60	7.56	9.67	11.21
Max. 1/2 h rainfall	45.07	32.73	33.70	46.03	42.17	22.70	17.67	12.57	18.10	28.83	49.63	52.13
Av. solar rad. (MJ/m^2)	20.60	21.20	20.96	18.46	16.22	16.79	16.94	18.18	20.60	22.05	21.43	21.06
Av. rel. humidity	0.64	0.62	0.68	0.73	0.68	0.59	0.56	0.55	0.54	0.57	0.63	0.65
Av. wind speed (m/s)	5.61	5.60	4.24	3.83	4.67	5.33	5.50	5.54	5.67	5.72	5.25	5.18

Agriculture (USDA) to simulate transportation of water, sediment, and agricultural nutrients at a watershed scale. The selection of SWAT in this study was due to its computational capability and robustness in incorporating weather, vegetation properties, topography, soil properties, and land management practices in the modeling. Also, SWAT has been widely applied in a significant number of studies to simulate and investigate hydrological responses of watersheds in different parts of the globe across varying climatic conditions and ecosystems (Ghoraba 2015; Narsimlu *et al.* 2015; Dile *et al.* 2016; Wang *et al.* 2019). More recently in Tanzania, the SWAT model has been successfully applied by Naschen *et al.* (2019), Kishiwa *et al.* (2018), and Alemayehu *et al.* (2017) to study hydrological responses of several catchments in the country.

Within SWAT, the SCS-CN method was co-implemented with other methods such as the Penman–Monteith for estimation of evapotranspiration (Monteith 1965) and the variable-rate storage method for streamflow (channel flow) routing. SWAT computes the water balance from the soil profile, snow, shallow aquifer, deep aquifer, and canopy storages. The overall water balance is estimated by SWAT using Equation (4). More theoretical and computational details of SWAT can be found at http://swat-model.tamu.edu/.

$$\Delta S = \sum_{i=1}^{N} (P - Q_{\text{total}} - \text{ET} - \text{losses})_i \tag{4}$$

where ΔS is the change in water storage (mm), P is the precipitation amount (mm), Q_{total} is the aggregate sum of water yield including surface runoff, lateral flow, and return flow, ET is the evapotranspiration (mm), *losses* represent groundwater losses, while i and N are indices representing the time steps (i.e. sub-daily, daily, etc.).

Model sensitivity analysis, calibration, and validation

In this study, the Soil and Water Assessment Tool Calibration and Uncertainty Program (SWAT-CUP) version 5.1.4 of 2012 was used to perform parameter sensitivity analysis, calibration, and validation of the SWAT model (Abbaspour 2015). The Sequential Uncertainty Fitting version 2 (SUFI-2) module was applied among five options available for uncertainty analysis within SWAT-CUP. SUFI-2 was opted for mainly due to its wide applicability in previous studies of hydrological modeling using SWAT (Khalid *et al.* 2016; Sao *et al.* 2020). A detailed description of these modules can be found in Abbaspour (2015). Based on the literature, there are more than 60 parameters in the SWAT model that can be used for model calibration depending on their usefulness in the runoff generation process (Ndomba *et al.* 2008). Some parameters represent physical field properties, e.g. channel width and depth; these were estimated directly from the available data using the GIS interface of the SWAT model. Many other parameters are empirical or SWAT-specific. More than 20 empirical parameters, which are related to soil properties, groundwater processes, runoff generation, and hydrology, were subjected to a parameter screening process to determine the most sensitive parameters that account for the runoff generation process. The parameter screening process finally retained four (4) most sensitive parameters for model calibration.

Like most urban catchments in Tanzania, the study area lacks recently observed streamflow data. The KZ-1J5 and MZ-1J6 stations had historical records of observed daily streamflow data of only four (4) years for the period 1969–1972, while the MS-KDJ station had no record of streamflow data at all. Historical observed streamflow data from the MZ-1J6 station was found to be of poor quality and was deemed unfit for model calibration; therefore, it was discarded. The SWAT rainfall-runoff model was then calibrated and validated using the observed historical daily streamflow hydrographs from the station KZ-1J5 of the Kizinga subcatchment. The available historical observed streamflow records were split into two sets, one for calibration (1969–1970) and the other for validation (1971–1972). Owing to spatial proximity and similarities in catchment characteristics of the studied subcatchments, the four (4) calibrated model parameters from the Kizinga subcatchment were transferred to the Msimbazi and Mzinga subcatchments and were used to generate streamflow data for the entire period as rainfall records. This approach of transferring model parameters of gauged catchments to ungauged ones and generate streamflow records has been previously successfully applied by Gandry *et al.* (2013) and Valimba (2019).

SUFI-2 uses several standard model performance metrics to quantify the goodness of fit between the simulated and observed data. Four commonly used model performance metrics were applied in this study to evaluate the agreement between the simulated and observed data and measure the model performance during model calibration and validation, these metrics included the percent bias (PBIAS), the root mean square error to the standard deviation ratio (RSR), the coefficient of determination (R^2), and the Nash–Sutcliffe Efficiency (NSE). The mathematical equation of each of the applied

model performance metrics are presented below:

$$\text{PBIAS} = \left(\frac{\sum_{i=1}^{N} (O_i - S_i)}{\sum_{i=1}^{N} O_i} \right) \times 100 \tag{5}$$

$$R^2 = \frac{\left[\sum_{i=1}^{N} (O_i - \bar{O})(S_i - \bar{S}) \right]^2}{\sum_{i=1}^{N} (O_i - \bar{O})^2 \sum_{i=1}^{N} (S_i - \bar{S})^2} \tag{6}$$

$$\text{NSE} = 1 - \frac{\sum_{i=1}^{N} (O_i - S_i)^2}{\sum_{i=1}^{N} (O_i - \bar{O})^2} \tag{7}$$

$$\text{RSR} = \frac{\sqrt{\sum_{i=1}^{N} (O_i - S_i)^2}}{\sqrt{\sum_{i=1}^{N} (O_i - \bar{S})^2}} \tag{8}$$

where S is the simulated variable, O is the observed variable, $\bar{O}$ is the mean of O, $\bar{S}$ is the mean of S, N is the total number of observations, and i is an index for events (observations).

Impact investigation scenarios

Some scenarios were developed while attempting to investigate and clearly understand the separate and combined effects of land-cover and climate changes on flood runoffs in the study area. The developed scenarios are presented in Table 2. It can be observed from Table 2 that some scenarios can be considered as totally hypothetical, while others as actual (or close to actual). In reality, the impacts of land cover and climate are happening simultaneously, therefore, any scenario that attempts to represent the independent effect of either climate or land-cover change can be considered as a hypothetical scenario. Therefore, the hypothetical scenarios were developed for the sole purpose of investigating and understanding the independent effects of land-cover and climate changes on urban flood runoffs. From Table 2, it can be seen that only two scenarios can be considered as actual, i.e. PB and PS3/FB. The remainder of the scenarios is hypothetical, including PS1, PS2, FS1, FS2, and FS3. As stipulated above, they are labeled as hypothetical because either they try to represent the independent effects of climate or land cover, and/or they try to predict what will happen in the future (considering the futuristic climate uncertainties). The actual scenarios represent the combined impacts of climate and land-cover changes while attempting to utilize more realistic climate and land-cover data. For the FS3 scenario, an average value of peak flow magnitudes was

Table 2 | Description of land-cover and climate change scenarios as applied in the analysis

Scenarios		Climate data	Land-cover map
Past Scenarios (1969–2017)	Past baseline scenario (PB)	1969–1993	1979
	Fixed climate and varied land-cover scenario (PS1)	1969–1993	2014
	Fixed land-cover and varied climate scenario (PS2)	1994–2017	1979
	Combined scenario of land-cover and climate change (PS3)	1994–2017	2014
Future Scenarios (2018–2050)	Future baseline scenario (FB)	1994–2017	2014
	Fixed climate & varied land-cover scenario (FS1)	1994–2017	2030
	Fixed land-cover and varied climate scenario (FS2)	2018–2050	2014
	Combined scenario of land-cover and climate change (FS3)	2018–2050	2030/2046

used, estimated using the projected land-cover scenarios of 2030 and 2046. This was done in order to obtain a more realistic representative figure for the future scenario, considering the wide range of climatic data.

Trend and frequency of flood runoff

It was of interest to investigate the separate and combined effects of land-cover and climate changes on the significance and magnitudes of long-term linear trends of flood runoff using the scenarios developed in the previous section. The Theil-Sen's slope estimator (Sen 1968) and Mann–Kendall (MK) method (Mann 1945; Kendall 1975) were used to test for changes in the magnitudes and significance of long-term linear trends of flood runoff, respectively. Moreover, it was also of interest to learn the impacts of land-cover and climate changes on the frequencies of flood runoff in the study area under similar scenarios. Based on the goodness of fit of the flood runoff time series to the Generalized Pareto (GP) distribution, the GP distribution (Pickands 1975) was used to model the frequencies of flood runoffs in this study. Flood runoff time series used in the assessment of trends of flood runoffs contained annual and seasonal peak floods in yearly and seasonal blocks (yearly and seasonal block maxima) under each studied scenario. Flood runoff time series used in modeling the frequencies of flood runoffs contained values that were equal and above a threshold of 20 m^3/s. This was determined to be the lower boundary of peak flows in the study area by using the box plot technique. The peak over threshold method was preferred over the block maxima method when modeling the frequencies of flood runoffs since it produced a longer time series and therefore increased the modeling accuracy. The methods discussed in this section are described in detail by Mzava *et al.* (2020), including their merits and shortcomings relative to other methods that could be used to perform similar tasks.

RESULTS AND DISCUSSION

Model parameter screening

The sensitivity analysis and parameter screening process identified four (4) most sensitive parameters (Table 3) that were then used in the model calibration and validation. These parameters were adjusted within the allowable range to obtain optimum parameter values for a satisfactory agreement between the observed and simulated daily streamflow values. Results of parameter screening indicated that the curve number (CN2) parameter was identified as the most important parameter in the runoff generation process in this study. The ranks of the other three parameters in the order of their importance to the runoff generation and hydrological processes, including their fitted values as applied in this study, are shown in Table 3.

Model calibration and validation

The visual interpretation of the graphical comparison between observed and simulated daily streamflow hydrographs of the calibration and validation scenarios (Figure 3) indicated a reasonable fit of the hydrographs in terms of the general flow pattern and magnitudes. However, due to the typical flow behavior of the streams in the study area, which are characterized by extreme low to zero flows during dry seasons and extreme high flows during the wet seasons, it can be seen from Figure 3 that the model struggled to balance between these extreme flow behaviors. It is evident from Figure 3 that the model slightly underestimated the low flows and also slightly overestimated the peak flows. The results of the model performance metrics (Table 4) also supported the reasonable performance of the model as indicated by the graphical interpretation of the observed and simulated streamflow hydrographs. Generally, a model can be judged to have performed satisfactorily if $R^2 > 0.5$, NSE

Table 3 | Identified most sensitive parameters used in the model calibration and validation

Parameter	Description	Unit	Min–Max range	Process	Fitted value	Ranking
CN2	SCS runoff curve number (for moisture condition 2)	–	35–98	Runoff generation	70.51*	1
ESCO	Plant uptake compensation factor	–	0–1	Evaporation	0.7	2
Sol_AWC	Available water capacity of the soil layer	mm H_2O/mm soil	0–1	Soil	0.38	3
Alpha_bf	Baseflow alpha factor	day	0–1	Groundwater	0.31	4

*Initial CN value fitted during the calibration period.

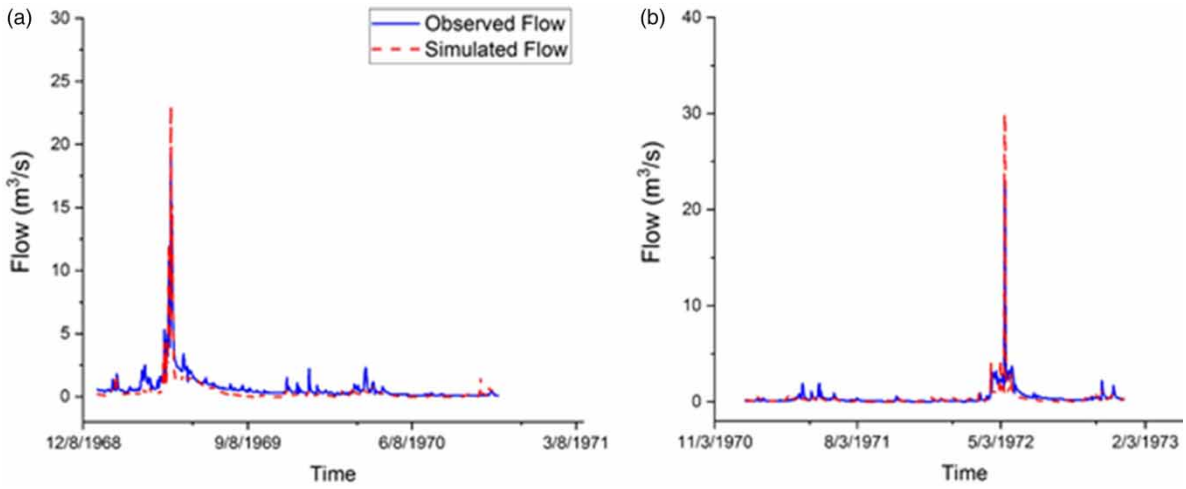

Figure 3 | Comparison of hydrographs of observed and simulated daily streamflows during (a) calibration and (b) validation.

Table 4 | Model performance metrics during calibration and validation

		Performance index			
Period		**NSE**	**R^2**	**RSR**	**PBIAS**
Calibration	Jan 1969–Dec 1970	0.71	0.88	0.51	18.7
Validation	Jan 1971–Dec 1972	0.63	0.79	0.42	15.6

>0.5, RSR ≤ 0.7, and if PBIAS $\pm 25\%$ for streamflow (Moriasi *et al.* 2007). Based on these guidelines of model performance and the performance metrics presented in Table 4, it can be concluded that the model performed satisfactorily.

Impacts of climate and land-cover changes on peak flow magnitudes

Figures 4 and 5 illustrate the separate and combined effects of climate and land-cover changes on peak flow magnitudes for the past and future scenario, respectively. Looking at the line joining the mean peak flow values under different scenarios, it can be observed that, independently, the effect of climate change (PS2, FS2) on peak flows is more profound compared with that of land-cover change (PS1, FS1). Also, it was observed that the combined effects of climate and land-cover changes (PS3, FS3) on peak flow magnitudes are much greater than the separate effects. In an attempt to further quantify the independent and combined impacts of climate and land-cover changes on flood magnitudes, changes in mean peak flow values from the baseline scenario were calculated and compared (Table 5). Table 5 also shows the mean peak flow values for different scenarios. On average, the percent change in mean peak flows was found to be $+35.48$, $+57.62$, and $+102.8\%$ when considering land-cover change alone, climate change alone, and the combined scenario, respectively, during the past scenario. Similarly, for the future scenario, these changes were estimated to be $+18.68$, $+19.86$, and $+44.46\%$, respectively. The changes in mean peak flow values were observed to be much higher in the past scenario compared with the future scenario. This is because, despite the future flood magnitudes being higher than those of the past, the variations in future flood magnitudes are less compared with those of the past. Similarly, as it was observed previously, climate change has a greater impact on change in peak flows than land-cover change when the two are treated separately in theory. Moreover, their combined effects cause a much bigger impact on the change in peak flows than any separate scenario. It must also be stressed that the combination of climate and land-cover changes represents the actual scenario on the ground.

Impacts of climate and land-cover changes on flood runoff frequencies

Estimated return periods of flood runoff in the study area based on the developed scenarios of land-cover and climate changes are shown in Table 6. The MZ-1J6 station showed to have recorded floods of much bigger magnitudes compared with MS-KDJ and KZ-1J5 stations, this is mainly due to the larger size of the drainage area upstream of the MZ-1J6 compared with the

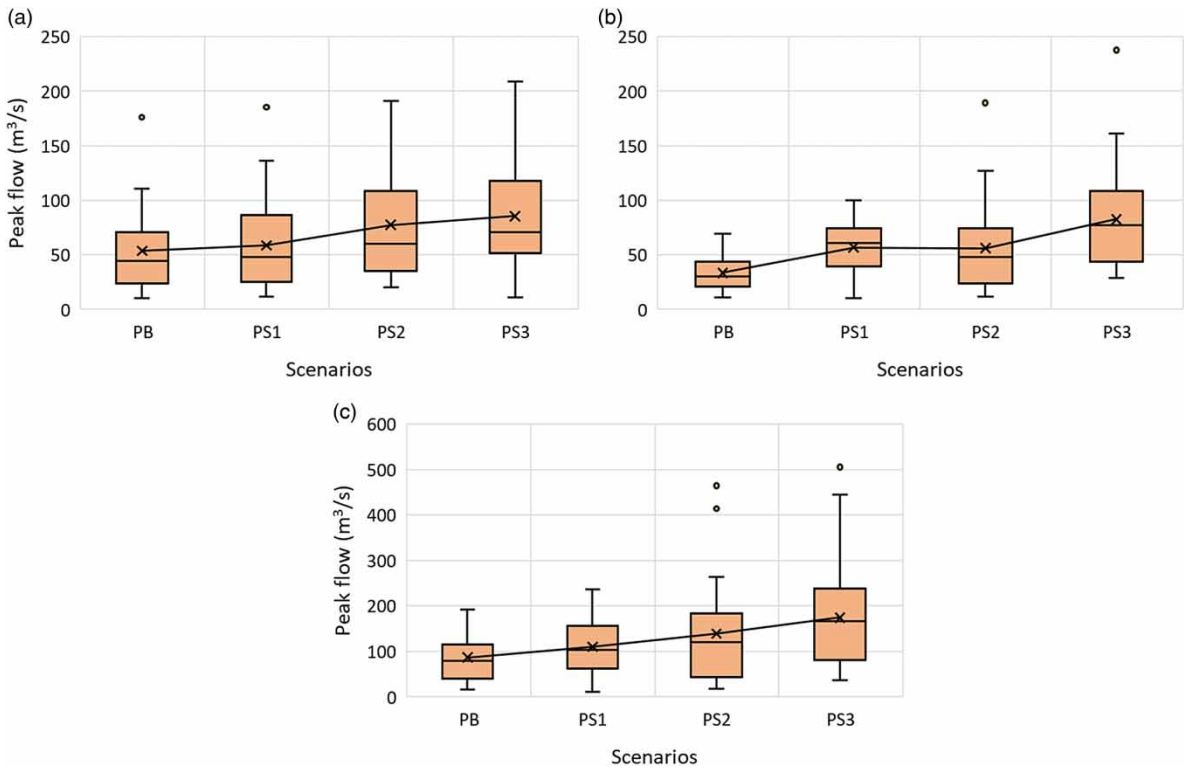

Figure 4 | Variation of peak flow values under different scenarios between 1969 and 2017 for (a) MS-KDJ, (b) KZ-1J5, and (c) MZ-1J6.

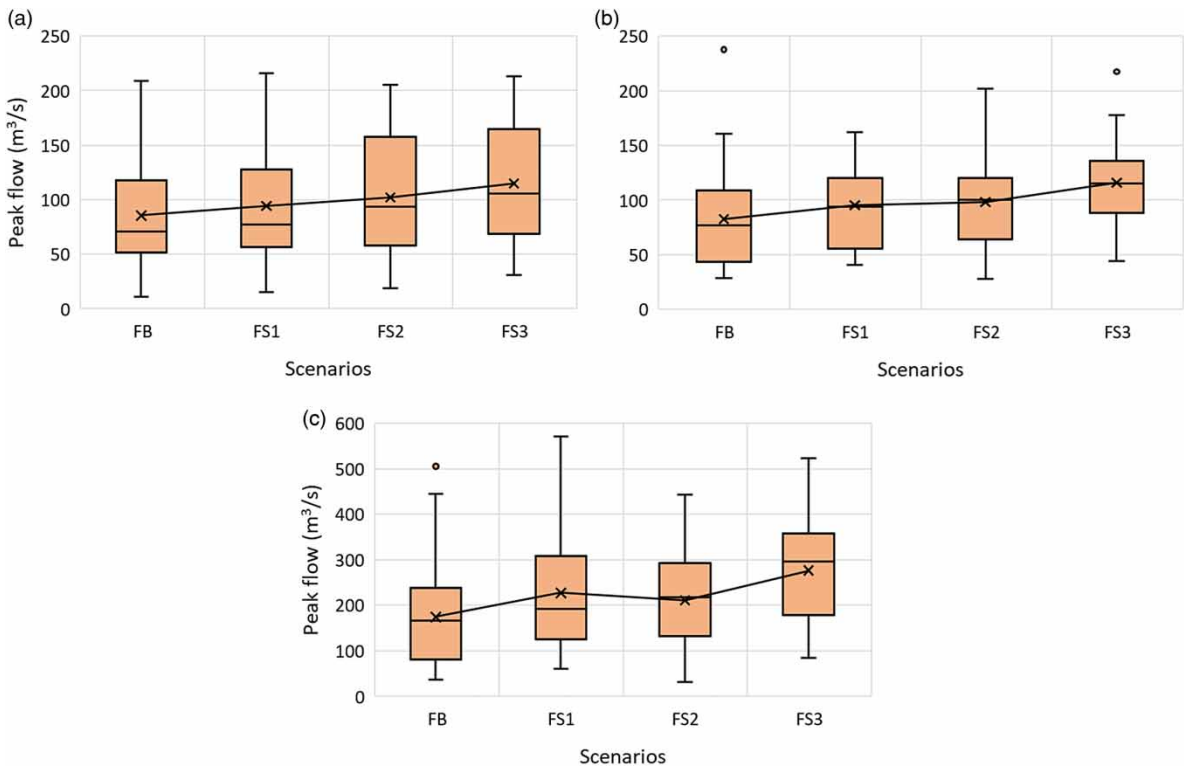

Figure 5 | Variation of peak flow values under different scenarios between 2018 and 2050 for (a) MS-KDJ, (b) KZ-1J5, and (c) MZ-1J6.

Table 5 | Variations of mean peak flows (Qe) under different scenarios

	MS-KDJ		KZ-1J5		MZ-1J6	
Scenarios	Mean Qe (m^3/s)	Change in Qe (%)	Mean Qe (m^3/s)	Change in Qe (%)	Mean Qe (m^3/s)	Change in Qe (%)
PB	53.53	–	33.33	–	86.57	–
PS1	58.44	9.17	56.76	70.30	109.92	26.97
PS2	77.44	44.67	55.96	67.90	138.76	60.29
PS3	85.42	59.57	82.51	147.55	174.18	101.20
FB	85.42	–	82.51	–	174.18	–
FS1	94.10	10.16	95.24	15.43	227.22	30.45
FS2	102.16	19.60	98.06	18.85	211.00	21.14
FS3	114.81	34.41	115.83	40.38	276.21	58.58

MS-KDJ and KZ-1J5 which have relatively smaller drainage areas. Generally, looking at the changes in flood runoff return periods of different scenarios, it was noticed that the differences in flood magnitudes of the scenarios are marginal for lower return periods and they become substantial for higher return periods. Also, similarly to what was observed previously when studying the variations of flood runoff magnitudes from independent impacts of land-cover and climate changes, it was observed here (Table 6) that climate has a higher impact on the frequencies of flood runoffs than land-cover change. These results are in agreement with the findings of previous studies on a similar subject from different parts of the globe. Chen & Yu (2015) concluded that climate changes have greater impacts on the magnitudes and frequency of floods than land-use changes from a study conducted in southeast Queensland, Australia. Similarly, a study by Poelmans *et al.* (2011) and Akter *et al.* (2018) in Belgium also suggested that climate change was likely to cause a larger change in peak flows compared with the studied scenarios of urban expansion. However, these results contradict the findings of Rukundo & Dogan (2016), who suggested that land-use change impacts predominate the climate change impacts in overall assessment on flood peaks in Kigali, Rwanda.

In quantitative terms, looking at Table 6, a 25-year flood runoff, for example, the ratio of climate only to land-cover only flood magnitudes is in the range 1.13–1.20 in the past and 1.02–1.21 in the future. The increase in flood runoff magnitudes brought by climate change relative to that of land-cover change implies that there is more increase in flood recurrence brought by climate change than land-cover change. For instance, from Table 6, a 25-year climate only flood event of 139 m^3/s from MS-KDJ in the past scenario can be approximated as a 37-year land-cover only event. In probabilistic terms, in any flooding event, there is a 0.04 (4%) chance that a 139 m^3/s flood magnitude may be exceeded when considering climate change alone. This probability is reduced to 0.027 (2.7%) when considering land-cover change alone. Therefore, when treating climate and land-cover changes separately, in the past, the probability of occurrence of urban flooding in the study area was likely to be increased up to 1.5-fold by climate change relative to land-cover change. In the future, this figure is estimated to decrease to 1.1-fold.

The difference in the probability of occurrence of flood runoffs from the separate and combined effects of climate and land-cover changes was observed to be more noticeable in the past than will be in the future, as it is depicted in Figure 6. It can be observed that the overall probability of occurrence of flood runoffs from the combined effects of climate and land-cover changes will increase in the future relative to the past, but the relative change from the separate impacts of climate and land-cover was more profound in the past than in the future. This can also be observed in Figure 7, where the change in peak flows as a function of the return period were determined to be marginal in the future irrespective of the increase in the return period. In the past, however, the change in peak flows as a function of the return period was observed to be significant and increasing with the increase of the return period. From Figure 7, the highest change in peak flows was observed to be imparted by the combined effects of climate and land-cover changes. In the past, this change (calculated as a ratio to baseline scenario) was determined to be in the range 1.25–1.92, 1.22–2.34, and 1.04–3.67 for MS-KDJ, KZ-1J5, and MZ-1J6, respectively. While in the future, this change is determined to be in the range 0.99–1.11, 1.13–1.28, and 1.23–1.53 for MS-KDJ, KZ-1J5, and MZ-1J6, respectively. From these numbers, it can be concluded that, on average, the change in peak flows from

Table 6 | Peak flows recurrence intervals under different scenarios

Scenarios	Return period (years)																	
	2			5			10			25			50			100		
PB	23	**18**	*35*	45	**31**	*73*	66	**44**	*108*	102	**65**	*165*	137	**84**	*218*	180	**108**	*279*
PS1	23	**19**	*29*	46	**35**	*72*	71	**52**	*128*	116	**84**	*254*	164	**118**	*415*	227	**163**	*670*
PS2	23	**19**	*31*	50	**38**	*79*	79	**58**	*142*	139	**99**	*286*	206	**144**	*474*	302	**209**	*776*
PS3	29	**22**	*36*	64	**46**	*97*	101	**72**	*177*	171	**121**	*366*	246	**176**	*617*	346	**252**	*1,025*
FB	29	**22**	*36*	64	**46**	*97*	101	**72**	*177*	171	**121**	*366*	246	**176**	*617*	346	**252**	*1,025*
FS1	28	**22**	*36*	63	**47**	*99*	102	**74**	*186*	177	**127**	*404*	260	**187**	*706*	375	**270**	*1,222*
FS2	30	**25**	*38*	67	**55**	*111*	106	**88**	*216*	180	**151**	*487*	259	**220**	*878*	364	**315**	*1,568*
FS3	29	**28**	*44*	65	**61**	*128*	104	**94**	*243*	181	**152**	*525*	266	**210**	*915*	385	**284**	*1,572*

Note: MS-KDJ, **KZ-1J5**, *MZ-1J6*.

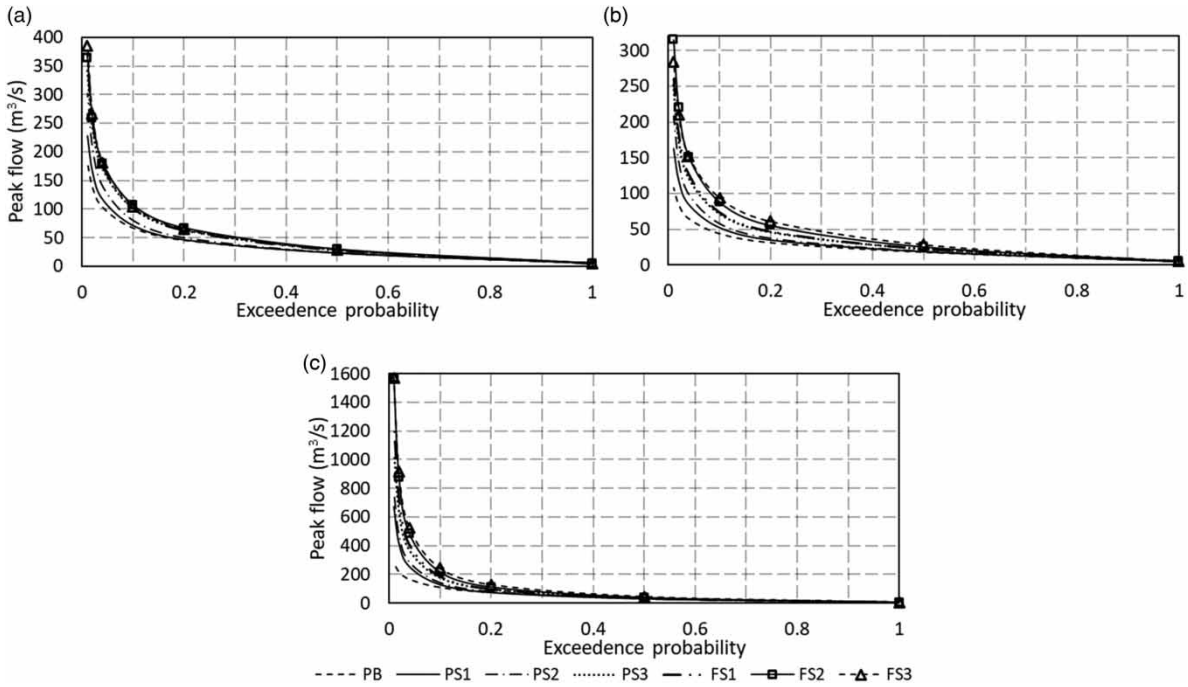

Figure 6 | Variations in the probabilities of peak flows under different scenarios of climate and land-cover changes for (a) MS-KDJ, (b) KZ-1J5, and (c) MZ-1J6.

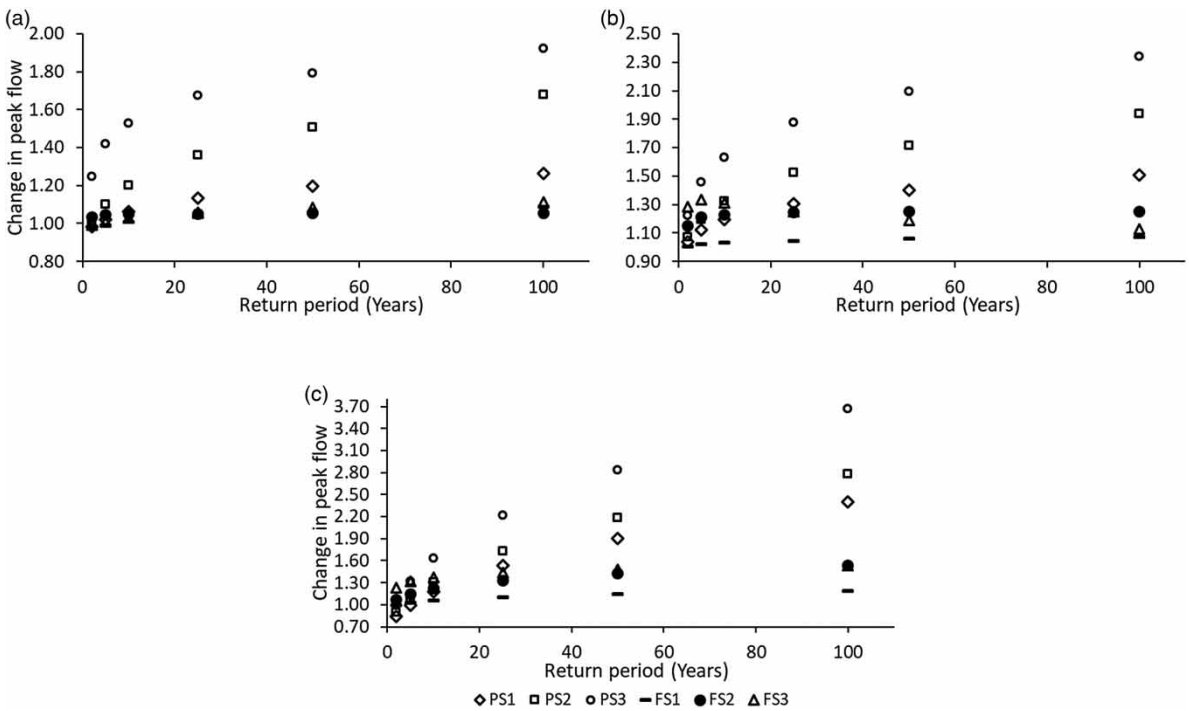

Figure 7 | Changes in peak flows as a function of return periods under different scenarios for (a) MS-KDJ, (b) KZ-1J5, and (c) MZ-1J6.

the combined effects of climate and land-cover changes will decrease by 36.3% in the future relative to the past. However, this decrement does not entail a decrease in flood magnitudes in the future, but rather the lesser variations in climate and land-cover changes in the future compared with those of the past. The magnitudes of mean peak flows (Table 5) were determined

to increase between 34.4 and 58.6% in the future relative to the past (from the combined effects of climate and land-cover changes). Similar to the findings of this study, Jiang *et al.* (2018) and Zhou *et al.* (2018) also projected an increase in urban flood risks as a result of climate change coupled with rapid land-use/cover changes.

Impacts of climate and land-cover changes on trends of flood runoff

It was of interest to study the behavior of annual and seasonal flood runoff trends under different scenarios of climate and land-cover changes. Tables 7 and 8 show the results of trend significance and magnitudes of the respective annual and seasonal peak flows under different scenarios. It can be observed from Table 7 that in the past, the trends of peak flows were determined to be statistically significant consistently under only two scenarios, i.e. the land-cover change alone scenario and the combined effect scenario. In the future, the statistical significance of the trends of peak flows could not be consistently determined under any scenario, therefore, the results were considered to be statistically indeterminate. From the overall assessment, however, the long-term trends (1969–2050) of both seasonal and annual peak flows, under the combined effects of climate and land-cover changes, were determined to be statistically increasing with some very strong *Z*-significance signals (see the last row of Table 7). The overall increase of long-term peak annual and seasonal flows in the study area was observed to be in the magnitudes of between 1.51–4.01 and 0.44–3.47 m^3/s, respectively (see the last row of Table 8). Considering rainfall as a major factor in runoff generation, Luhunga *et al.* (2018) projected an increase of rainfall almost throughout Tanzania. More specifically, Mzava *et al.* (2020) observed an overall significant increase in long-term annual maximum rainfall from all the studied stations in the urban catchments of Dar es Salaam and the *Masika* maximum rainfall from two stations located upstream of the studied catchments. The respective upstream catchment areas contribute to a major portion of the flood

Table 7 | MK trend test statistic *Z*-value for peak flows

		MS-KDJ			KZ-1J5			MZ-1J6		
Period	Scenarios	Annual Q_{max}	Masika Q_{max}	Vuli Q_{max}	Annual Q_{max}	Masika Q_{max}	Vuli Q_{max}	Annual Q_{max}	Masika Q_{max}	Vuli Q_{max}
1969–2017	Baseline	**3.15**	**2.50**	1.85	**2.03**	1.66	1.85	1.66	1.38	1.56
	Land-cover change alone	**3.50**	**3.15**	**3.57**	**4.33**	**3.71**	**4.99**	**3.01**	**2.51**	**3.20**
	Climate change alone	1.70	1.23	0.51	**2.16**	1.54	1.27	**2.09**	1.59	1.65
	Combined effect	**2.84**	**2.30**	**2.78**	**4.42**	**3.82**	**4.58**	**3.37**	**2.75**	**3.72**
2018–2050	Baseline	−1.91	−1.86	−0.37	−0.92	−1.27	−0.97	−0.67	−0.97	−0.27
	Land-cover change alone	−0.52	−0.90	0.96	0.50	−0.03	0.67	0.76	0.33	1.63
	Climate change alone	0.37	0.50	0.51	0.97	0.48	0.83	0.91	0.76	0.00
	Combined effect	0.92	0.94	1.16	**2.09**	1.38	1.87	**2.29**	1.93	1.60
1969–2050	Combined effect	**4.68**	**4.54**	**4.04**	**6.70**	**6.00**	**6.35**	**5.81**	**5.33**	**5.23**

Note: Bold values indicate statistical significance at ≥95% confidence level (+ increasing; − decreasing).

Table 8 | Sen's slope trend magnitudes for peak flows

		MS-KDJ			KZ-1J5			MZ-1J6		
Period	Scenarios	Annual Q_{max}	Masika Q_{max}	Vuli Q_{max}	Annual Q_{max}	Masika Q_{max}	Vuli Q_{max}	Annual Q_{max}	Masika Q_{max}	Vuli Q_{max}
1969–2017	Baseline	**2.60**	**1.79**	0.29	**1.06**	0.8	0.24	3.28	2.24	0.39
	Land-cover change alone	**1.11**	**0.78**	**0.42**	**1.03**	**0.82**	**0.66**	**1.85**	**1.50**	**0.58**
	Climate change alone	0.74	0.49	0.01	**0.59**	0.40	0.05	**1.51**	1.03	0.17
	Combined effect	**1.30**	**0.96**	**0.23**	**1.39**	**1.13**	**0.69**	**2.60**	**2.20**	**1.08**
2018–2050	Baseline	−3.18	−3.96	−0.21	−1.32	−1.86	−0.89	−3.09	−3.90	−0.29
	Land-cover change alone	−0.34	−0.56	0.16	0.19	−0.04	0.22	0.99	0.41	1.23
	Climate change alone	0.15	0.24	0.12	0.46	0.24	0.23	1.31	1.03	0.00
	Combined effect	0.56	0.53	0.34	**1.00**	0.68	0.73	**3.58**	2.78	1.14
1969–2050	Combined effect	**1.51**	**1.30**	**0.44**	**1.72**	**1.41**	**0.94**	**4.01**	**3.47**	**1.34**

Note: Bold values indicate statistical significance at ≥95% confidence level (+ increasing; − decreasing).

runoff experienced by the downstream urban center of Dar es Salaam. However, for the case of peak flows in the current study, unlike the *Vuli* maximum rainfall which was observed to be significantly increasing only at the DIA station by Mzava *et al.* (2020), the *Vuli* maximum discharge was determined to be significantly increasing at all the studied flow gauging stations. This could be indicative of the influence of land-cover changes on the trend of flood runoffs.

Due to the observed significant increase in peak flow trend magnitudes, imparted by the combined effects of climate and land-cover changes, for the past scenario (1969–2017) and the overall study period (1969–2050) (see Table 8). It was of interest to learn the future increase in peak flow trend magnitudes relative to the past, under the same scenario. Figure 8 shows the relative future increase in annual and seasonal maximum discharges from the studied streamflow gauging stations. Based on the mean relative increase, the trend magnitudes of *Annual*, *Masika*, and *Vuli* maximum discharges will increase by 31.3, 39.3, and 50.3% in the future, respectively. These findings are consistent with what is currently starting to be experienced on the ground in the study area. Unusually, longer *Vuli* rainfalls and more flooding are now being experienced in the study area during the *Vuli* season contrary to what was being experienced in the past (where more floods were being experienced during the *Masika* season than *Vuli*). With the current flood experience in the study area, the difference between the two seasons is minimal. Therefore, based on the actual experience and the findings of this study, the separate and coupled impacts of climate and land-cover changes are becoming apparent. Particularly, on the contribution of land-cover changes on the trend of flood runoffs during the *Vuli* season as discussed in the previous section.

CONCLUSION

In an attempt to quantify the separate and combined impacts of climate and land-cover changes on urban flood runoffs in Dar es Salaam, Tanzania, SWAT hydrological modeling was performed while incorporating first the past climate and land-cover changes. Furthermore, future land-cover change scenario and projected climate change scenario obtained from the CORDEX-Africa regional climate model were then also incorporated in the modeling. A validated SWAT model was then used to simulated flood hydrographs under different past and future scenarios of climate and land-cover changes. Subsequently, a quantitative analysis of the impacts of climate and land-cover changes to flood runoffs in the urban catchments of Dar es Salaam was undertaken.

Results showed that climate change has a greater impact on change in peak flows than land-cover change when the two are treated separately in theory. It was observed that in the past the probability of occurrence of urban flooding in the study area was likely to be increased by up to 1.5-fold by climate change relative to land-cover change. In the future, this figure is estimated to decrease to 1.1-fold. The coupled effects of climate and land-cover changes cause a much bigger impact on change in peak flows than any separate scenario; this scenario represents the actual scenario on the ground. From the combined effects of climate and land-cover changes, the magnitudes of mean peak flows were determined to increase between 34.4 and 58.6% in the future relative to the past. However, the change in peak flows from the combined effects of climate and land-cover changes will decrease by 36.3% in the future relative to the past; owing to the lesser variations in climate and land-cover changes in the future compared with those of the past. The hydrological modeling in this study was carried out using daily climate inputs. Valimba & Mahe (2020) suggested the inability of hydrological models to simulate flood hydrographs

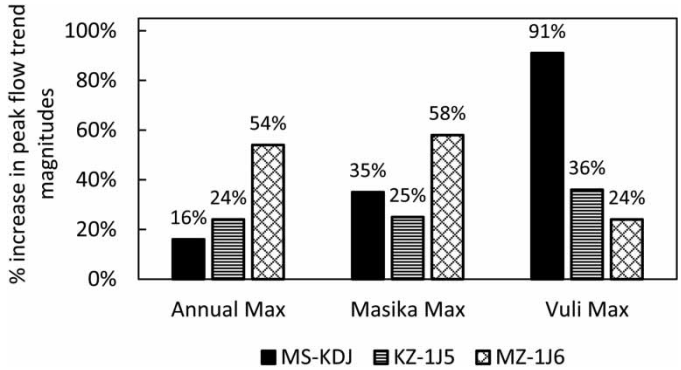

Figure 8 | Relative increase in peak flow trend magnitudes when considering the combined effects of land-cover and climate changes between past and future scenarios.

for fast draining urban catchments using daily climate inputs, due to the underestimation of flood peaks. Therefore, depending on data availability, further modeling and research work on the impacts of climate and land-use/cover changes on urban flood characteristics is recommended using sub-daily climate inputs, so as to have a much clearer perspective on the subject matter.

In conclusion, it was determined from this study that climatic changes have greater impacts on the magnitudes and frequency of flood runoffs in urban Dar es Salaam than land-cover changes. It is, therefore, recommended that much emphasis should be placed on future climate change and climate-related parameters during the design and practice of hydrologic engineering in the study area. In addition, consideration of land-cover change is equally important, as it was determined that the worst-case scenario from this study is imparted by the combination of climate and land-cover changes. Factoring in the land-cover changes is important considering the ongoing urban development and infrastructure upgrading in urban Dar es Salaam, and their direct and significant influences on urban flooding.

ACKNOWLEDGEMENTS

The authors appreciate the financial support for this research work from the German Academic Exchange Service (DAAD) through grant programme No. SFBFR2015-57220758.

CONFLICTS OF INTEREST

The authors declare no conflict of interest with regard to the publication of this paper.

DATA AVAILABILITY STATEMENT

All relevant data are included in the paper or its Supplementary Information.

REFERENCES

Abbaspour, K. C. 2015 *SWAT-CUP: SWAT Calibration and Uncertainty Programs – A User Manual*.

Abidin, H. Z., Andreas, H., Gumilar, I. & Wibowo, I. R. R. 2015 On the correlation between urban development, land subsidence and flooding phenomena in Jakarta. *IAHS-AISH Proceedings and Reports* **370**, 15–20. https://doi.org/10.5194/piahs-370-15-2015.

Akter, T., Quevauviller, P., Eisenreich, S. J. & Vaes, G. 2018 Impacts of climate and land use changes on flood risk management for the Schijn River, Belgium. *Environmental Science and Policy* **89**, 163–175. https://doi.org/10.1016/j.envsci.2018.07.002.

Alemayehu, T., Van Griensven, A., Woldegiorgis, B. T. & Bauwens, W. 2017 An improved SWAT vegetation growth module and its evaluation for four tropical ecosystems. *Hydrology and Earth System Sciences* **21**, 4449–4467. https://doi.org/10.5194/hess-21-4449-2017.

Arnold, J. G., Srinivasan, R., Muttiah, R. S. & Williams, J. R. 1998 Large area hydrologic modeling and assessment – Part I: model development. *Journal of the American Water Resources Association* **34**, 73–89. https://doi.org/10.1111/j.1752-1688.1998.tb05961.x.

Chen, Y. & Yu, B. 2015 Impact assessment of climatic and land-use changes on flood runoff in southeast Queensland. *Hydrological Sciences Journal* **60** (10), 1759–1769.

Dewitte, O., Jones, A., Spaargaren, O., Breuning-Madsen, H., Brossard, M., Dampha, A., Deckers, J., Gallali, T., Hallett, S., Jones, R., Kilasara, M., Le Roux, P., Micheli, E., Montanarella, L., Thiombiano, L., Van Ranst, E., Yemefack, M. & Zougmore, R. 2013 Harmonization of the soil map of Africa at a continental scale. *Geoderma* **211–212**, 138–153. https://doi.org/10.1016/j.geoderma.2013.07.007.

Dile, Y. T., Daggupati, P., George, C., Srinivasan, R. & Arnold, J. 2016 Introducing a new open source GIS user interface for the SWAT model. *Environmental Modelling and Software* **85**, 129–138. http://dx.doi.org/10.1016/j.envsoft.2016.08.004.

Emam, A. R., Mishra, B. K., Kumar, P., Masago, Y. & Fukushi, K. 2016 Impact assessment of climate and land-use changes on flooding behavior in the upper Ciliwung River, Jakarta, Indonesia. *Water* **8** (12), 559. https://doi.org/10.3390/w8120559.

Erman, A., Tariverdi, M., Obolensky, M., Chen, X., Vincent, R. C., Malgioglio, S., Rentschler, J., Hallegatte, S. & Yoshida, N. 2019 *The Role of Poverty in Exposure, Vulnerability and Resilience to Floods in Dae es Salaam*. World Bank Group. Available from: http://documents.worldbank.org/curated/pt/788241565625141093/pdf/Wading-Out-the-Storm-The-Role-of-Poverty-in-Exposure-Vulnerability-and-Resilience-to-Floods-in-Dar-Es-Salaam.pdf (accessed 20 December 2020).

Gandry, M., Gailliez, S., Sohier, C., Verstraete, A. & Degre, A. 2013 A method for low-flow estimation at ungauged sites: a case study in Walloni, Belgium. *Hydrology and Earth System Sciences* **17**, 1319–1330. https://doi.org/10.5194/hess-17-1319-2013.

Ghoraba, S. M. 2015 Hydrological modeling of the Simly Dam watershed (Pakistan) using GIS and SWAT model. *Alexandria Engineering Journal* **54** (3), 583–594. http://dx.doi.org/10.1016/j.aej.2015.05.018.

Hausfather, Z. & Peters, G. P. 2020 Emission – the 'business as usual' story is misleading. *Nature* **577** (7792), 618–620. https://doi.org/10.1038/d41586-020-00177-3.

Hlodversdottir, A. O., Bjornsson, B., Andradottir, H. O., Eliasson, J. & Crochet, P. 2015 Assessment of flood hazard in a combined sewer system in Reykjavik city center. *Water Science & Technology* **71** (10), 1471–1477. https://doi.org/10.2166/wst.2015.119.

Jiang, Y., Zevenbergen, C. & Ma, Y. C. 2018 Urban pluvial flooding and stormwater management: a contemporary review of China's challenges and 'sponge cities' strategy. *Environmental Science and Policy* **80**, 132–143.

Kebede, A. S. & Nicholls, R. J. 2011 *Population and Assets Exposure to Coastal Flooding in Dar es Salaam (Tanzania): Vulnerability to Climate Extremes Report*. Global Climate Adaptation Partnership (GCAP) Programme.

Kendall, M. G. 1975 *Rank Correlation Measures*. Charles Griffin, London.

Khalid, K., Ali, M. F., Rahman, N. F. A., Mispan, M. R., Haron, S. H., Othman, Z. & Bachok, M. F. 2016 Sensitivity analysis in watershed model using SUFI-2 algorithm. *Procedia Engineering* **162**, 441–447. https://doi.org/10.1016/j.proeng.2016.11.086.

Kishiwa, P., Nobert, J., Kongo, V. & Ndomba, P. 2018 Assessment of impacts of climate change on surface water availability using coupled SWAT and WEAP models: case of upper Pangani river basin, Tanzania. Presented at *the Proceedings of the International Association of Hydrological Sciences*, pp. 23–27. https://doi.org/10.5194/piahs-378-23-2018.

Luhunga, P. M., Kijazi, A. L., Chang'a, L., Kondowe, A., Ng'ongolo, H. & Mtongori, H. 2018 Climate change projections for Tanzania based on high-resolution regional climate models from CORDEX-Africa. *Frontiers in Environmental Science Journal* **6**, 122. https://doi.org/10.3389/fenvs.2018.00122.

Mahmoud, S. H. & Gan, T. Y. 2018 Urbanization and climate change implications in flood risk management: developing an efficient decision support system for flood susceptibility mapping. *Science of the Total Environment* **636**, 152–167.

Mahongo, S. B. & Khamis, O. I. 2006 *The Tanzania National Sea Level Report*. Tanzania Fisheries Research Institute and the Department of Survey and Urban Planning. Available from: http://www.gloss-sealevel.org/publications/documents/tanzania2006.pdf (accessed 09 November 2020).

Mallakpour, I. & Villarini, G. 2016 Analysis of changes in the magnitude, frequency, and seasonality of heavy precipitation over the contiguous USA. *Theoretical and Applied Climatology* **130**, 345–363. https://doi.org/10.1007/s00704-016-1881-z.

Mann, H. B. 1945 Non-parametric tests against trend. *Econometrica* **13**, 245–259.

Monteith, J. L. 1965 Evaporation and the environment. In: *The State and Movement of Water in Living Organisms*. Presented at *the XIXth Symposium*, Cambridge University Press, Swansea.

Moriasi, D. N., Arnold, J. G., Van Liew, M. W., Bingner, R. L., Harmel, R. D. & Veith, T. L. 2007 Model evaluation guidelines for systematic quantification of accuracy in watershed simulations. *American Society of Agricultural and Biological Engineers* **50** (3), 885–900.

Mzava, P., Nobert, J. & Valimba, P. 2019 Land cover change detection in the urban catchments of Dar es Salaam, Tanzania using remote sensing and GIS techniques. *Tanzania Journal of Science* **45** (3), 315–329.

Mzava, P., Nobert, J. & Valimba, P. 2020 Characterizing past and future trend and frequency of extreme rainfall in urban catchments: a case study. *H_2Open Journal* **3** (1), 288–305. https://doi.org/10.2166/h2oj.2020.009.

Narsimlu, B., Gosain, A., Chahar, B. R., Singh, S. K. & Srivastava, P. K. 2015 SWAT model calibration and uncertainty analysis for streamflow prediction in the Kunwari River Basin, India, using sequential uncertainty fitting. *Environmental Processes* **2**, 79–95.

Naschen, K., Diekkruger, B., Leemhuis, C., Seregina, L. S. & van der Linden, R. 2019 Impacts of climate change on water resources in the Kilombero catchment in Tanzania. *Water* **11** (4), 859. https://doi.org/10.3390/w11040859.

Ndomba, P., Mtalo, F. & Killingtveit, A. 2008 SWAT model application in a data scarce tropical complex catchment in Tanzania. *Physics and Chemistry of the Earth* **33**, 626–632. https://doi.org/10.1016/j.pce.2008.06.013.

Ngailo, T. J., Reuder, J., Rutalebwa, E., Nyimvua, S. & Mesquita, M. 2016 Modelling of extreme maximum rainfall using extreme value theory for Tanzania. *International Journal of Scientific and Innovative Mathematical Research* **4** (3), 34–45.

Notter, B., MacMillan, L., Viviroli, D., Weingartner, R. & Liniger, H. 2007 Impacts of environmental change on water resources in the Mt. Kenya region. *Journal of Hydrology* **343** (3), 266–278. https://doi.org/10.1016/j.jhydrol.2007.06.022.

Ouellet, C., Saint-Laurent, D. & Normand, F. 2012 Flood events and flood risk assessment in relation to climate and land-use changes: Saint-Francois River, southern Quebec, Canada. *Hydrological Sciences Journal* **57** (2), 313–325. https://doi.org/10.1080/02626667.2011.645475.

Pickands, J. 1975 Statistical inference using extreme order statistics. *Annals of Statistics* **3**, 119–131.

Poelmans, L., Rompaey, A., Ntegeka, V. & Willems, P. 2011 The relative impact of climate change and urban expansion on peak flows: a case study in central Belgium. *Hydrological Processes* **25** (18), 2846–2858. https://doi.org/10.1002/hyp.8047.

Ponce, V. M. & Hawkins, R. H. 1996 Runoff curve number: has it reached maturity? *Journal of Hydrologic Engineering* **1**, 11–19.

Rukundo, E. & Dogan, A. 2016 Assessment of climate and land use change projections and their impacts on flooding. *Polish Journal of Environmental Studies* **25** (6), 2541–2551. https://doi.org/10.15244/pjoes/63781.

Sao, D., Kato, T., Tu, L. H., Thouk, P., Fitriyah, A. & Oeurng, C. 2020 Evaluation of different objective functions used in the SUFI-2 calibration process in SWAT-CUP on water balance analysis: a case study of the Pursat river basin, Cambodia. *Water* **12**, 2901. https://doi.org/10.3390/w12102901.

Sen, P. K. 1968 Estimation of the regression coefficient based on Kendall's tau. *Journal of American Statistical Association* **63**, 1379–1389.

Soil Conservation Service (SCS) 1985 *National Engineering Handbook. Section 4: Hydrology*. US Department of Agriculture, Washington, DC.

Thanvisitthpon, N., Shrestha, S. & Pal, I. 2018 Urban flooding and climate change: a case study of Bangkok, Thailand. *Environment and Urbanization ASIA* **9**, 86–100.

Trzaska, S. & Schnarr, E. 2014 *A Review of Downscaling Methods for Climate Change Projections*. Tetra Tech ARD, USAID, Burlington, Vermont.

United States Department of Agriculture (USDA) 1972 *National Engineering Handbook – Section 4. Hydrology*. US Department of Agriculture, Washington.

Valimba, P. 2019 Development of improved characteristic equations for lake Rukwa in Tanzania. *Tanzania Journal of Engineering & Technology* **38** (1), 83–96.

Valimba, P. & Mahe, G. 2020 Estimating flood magnitudes of ungauged urban Msimbazi river catchment in Dar es Salaam, Tanzania. *Tanzania Journal of Engineering & Technology* **39** (1), 59–71.

Wakuma, A. S., Mandere, N. & Ewald, G. 2009 Floods and health in Gambella region, Ethiopia: a qualitative assessment of the strengths and weaknesses of coping mechanisms. *Global Health Action* **2**, 1–10.

Wang, J., Feng, L., Tang, X., Bentley, Y. & Hook, M. 2017 The implications of fossil fuel supply constraints on climate change projections: a supply-side analysis. *Futures* **86** (2), 58–72. https://doi.org/10.1016/j.futures.2016.04.007.

Wang, Y., Jiang, R., Xie, J., Zhao, Y., Yan, D. & Yang, S. 2019 Soil and water assessment tool (SWAT) model: a systemic review. *Journal of Coastal Research* **93**, 23–30. https://doi.org/10.2112/SI93-004.1.

Wu, X. S., Wang, Z. L., Guo, S. L., Liao, W., Zeng, Z. & Chen, X. 2017 Scenario-based projections of future urban inundation within a coupled hydrodynamic model framework: a case study in Dongguan City, China. *Journal of Hydrology* **547**, 428–442.

Yazd, H. R. G., Salehnia, N., Kolsouni, S. & Hoogenboom, G. 2019 Prediction of climate variables by comparing the K-nearest neighbor method and MIROC5 outputs in an arid environment. *Climatic Research* **77**, 99–144.

Zhou, Q. Q., Leng, G. Y. & Huang, M. Y. 2018 Impacts of future climate change in urban flood volumes in Hohhot in northern China: benefits of climate change mitigation and adaptations. *Hydrology and Earth System Sciences* **22**, 305–316.

First received 18 January 2021; accepted in revised form 15 May 2021. Available online 14 June 2021